JOURNAL OF SOLID STATE CHEMISTRY 85, 23–30 (1990)

Dehydration Reactions of Gypsum: A Neutron and X-Ray Diffraction Study

W. ABRIEL* AND K. REISDORF

Institut für Anorganische Chemie und SFB 173 der Universität, Hannover, Callinstrasse 9, D-3000 Hannover 1, Federal Republic of Germany

AND J. PANNETIER

Institut Laue-Langevin, F-38042 Grenoble CEDEX, France

Received March 6, 1989; in revised form October 27, 1989

The kinetics of the dehydration of gypsum was investigated by powder diffraction methods. Using the incoherent scattering effect of H with the neutron beam, the background intensity as a measure of the water content was checked in the temperature range 295–623 K. The superposed Bragg peaks yielded four major phases: Gypsum, subhydrates $CaSO_4(H_2O)_x$ $(1 > x > 0)$, AIII-$CaSO_4$, AII-$CaSO_4$. For the subhydrates a maximum water content of $x = 0.74$ was determined. A different kinetic was found using Guinier X-ray technique with the heated sample prepared on a thin foil. Only with high local H_2O steam pressure, produced in the comparable larger sample container of the neutron diffraction experiment, could this high H_2O occupation of the subhydrate tunnel structure be found. A topotactic mechanism can describe the phase transitions for this reaction. © 1990 Academic Press, Inc.

Introduction

Although the dehydration reaction of gypsum is a very important technical process, only little is known about the reaction mechanism and the water content of the corresponding phases. In the course of a more general investigation of the reactions in the system $CaSO_4(H_2O)_2$–$CaSO_4$ (*1*), this work reports results of a powder diffraction study of the thermal decomposition of gypsum.

With this dry thermal dehydration the β-plasters (*2*) are formed containing subhydrates $CaSO_4(H_2O)_x$ $(1 > x > 0)$, AIII-$CaSO_4$ (soluble anhydrite), and AII-$CaSO_4$ (anhydrite) in different amounts. Among the subhydrates, the hemihydrate $CaSO_4(H_2O)_{0.5}$ is considered to be the kinetically most stable phase. According to different authors (*3–6*), higher H_2O contents for these subhydrates should occur beyond the hemihydrate stage. On the other hand, Lager *et al.* (*7*) rejected all considerations on water contents higher than $CaSO_4(H_2O)_{0.5}$.

The following questions will be answered by our experiments:

1. Are there any new phases $CaSO_4(H_2O)_x$ $(2 > x > 1)$ between gypsum and the subhydrates?

* To whom correspondence should be addressed at present address: Institut für Anorganische Chemie der Universität, P.O. Box 397, D-8400 Regensburg, FRG.

0022-4596/90 $3.00
Copyright © 1990 by Academic Press, Inc.
All rights of reproduction in any form reserved.

2. What is the maximum water content of a subhydrate?

From DTA or TG measurements in the range $CaSO_4(H_2O)_x$ ($2 > x > 0$) one can get a signal for the kinetically most stable phase, the hemihydrate, exclusively (*1*, *8*). As all these kinetically controlled transitions are of first order, an averaging probe (like DTA/TG) is not suitable for detecting distinct phases coexisting with others.

The use of powder diffraction methods with the combination of a high neutron flux and multichannel detectors has made it possible to investigate chemical reactions by on-line neutron diffraction for somewhat faster reactions (*9*). Neutron Thermodiffractometry (NTD) can be considered one of the many experimental techniques for studying thermally stimulated processes.

The high incoherent background from hydrogenous samples is usually considered as very inconvenient in neutron powder diffraction in that it severely decreases the quality of the pattern (peak to background ratio). This inconvenience still exists in NTD experiments but it can sometimes be seen as an advantage because this incoherent scattering provides a straight-forward measure of the proton content of the material under investigation (*10*). This affords the possibility of investigating simultaneously the composition (proton or water content, respectively) and structural characteristics of the sample.

Experimental

Starting material for the diffraction experiments was powdered gypsum (Merck, Art. No. 2161) sieved to particle size less than 50 μm.

In the neutron diffraction experiments about 5 g of this powder was given compactly into a cylindrical vanadium container (10 mm diameter, 80 mm height). The neutron diffraction powder pattern was recorded at the diffractometer D1B of the Institute Laue-Langevin with the container placed in a thermostated vanadium oven with a temperature stability of 1 K. For more experimental details see Table I.

The X-ray powder diffraction experiment was performed with a modified temperature-controlled Guinier diffractometer (*11*) using Ge-monochromatized Cu$K\alpha_1$ radiation. The powder was prepared on a 0.02-mm-thick Al-sputtered Mylar foil. The dehydration reaction at a constant temperature of 335(1) K was recorded with 10 diffractograms in time intervals of 12 min (θ range 5–25°). Starting at ambient temperature, the 335 K level was reached in about 5 min.

Results

Figure 1 shows the three-dimensional array of the neutron diffraction pattern indicating the kinetics of the dehydration reaction. Starting phase at ambient temperatures is gypsum (Bragg peaks on high background intensity). With increasing temperature, the intensities of the gypsum peaks decrease, paralleling the decrease of the background intensity. A new pattern, associated with the subhydrate structure,

TABLE I

EXPERIMENTAL DETAILS OF THE NEUTRON POWDER DIFFRACTION EXPERIMENT

Wavelength	2.517 Å
Monochromator	Graphite (002)
2θ min/max (°)	11/91
Zero shift in 2θ (°)	0.2
T min/max (K)	295/623
Heating rate (K/min)	0.15
Time interval for diffraction patterns (min)	5
Number of patterns	542
Neutron flux at the sample (n/cm^2/sec)	$1.6 \cdot 10^6$
Vacuum at the sample (begin/end) (bar)	$2.5/1.0 \cdot 10^{-4}$

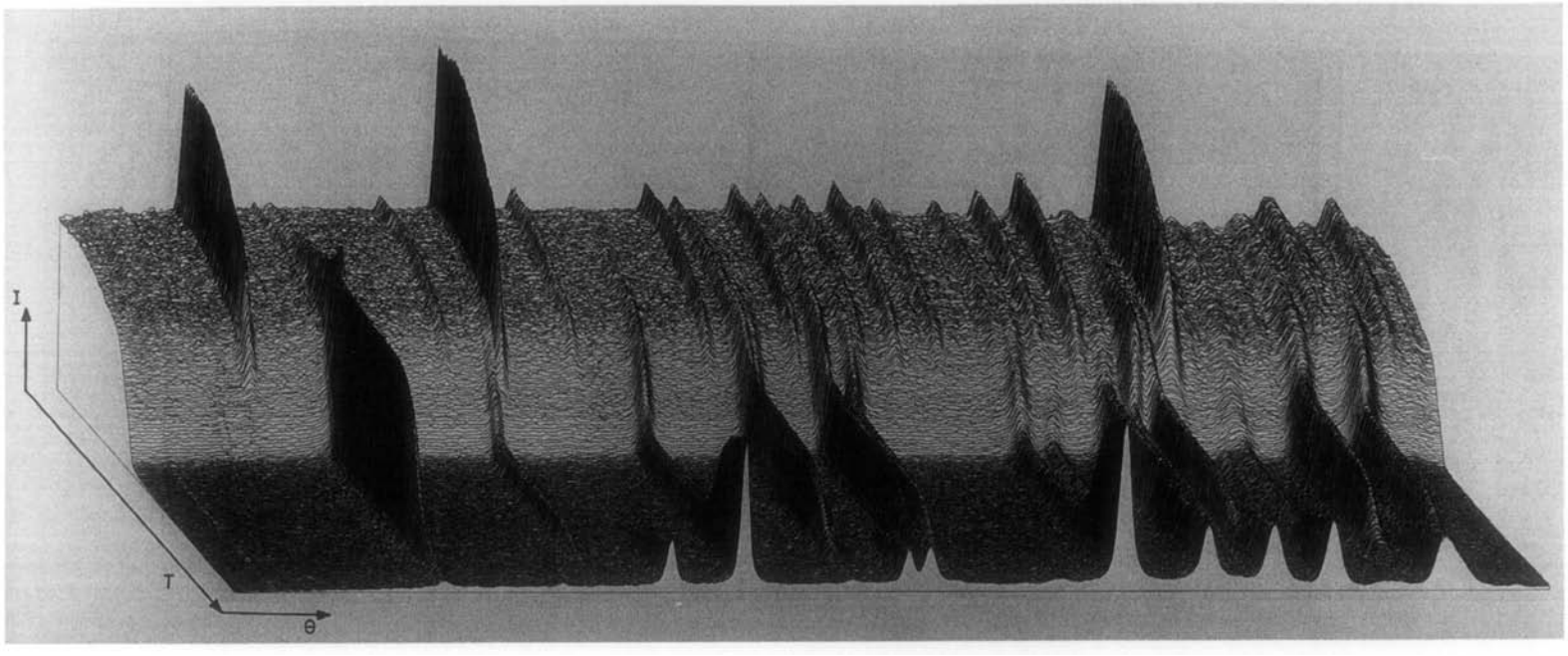

FIG. 1. Three-dimensional array of the neutron diffraction patterns. Diffraction angle θ from 11 to 91° (λ = 2.517 Å).

TABLE II

DATA OF THE GRAPHICAL EVALUATION FROM FIGURES 2 AND 3

% gypsum	Water from gypsum	Overall water	Subhydrate water	% subhydrate	x for subhydrate $CaSO_4(H_2O)_x$
100	2	2	—	—	—
90	1.8	1.85(2)	0.05(2)	10	0.46(20)
80	1.6	1.71(2)	0.11(2)	20	0.53(10)
70	1.4	1.60(2)	0.20(2)	30	0.66(7)
65	1.3	1.56(1)	0.26(1)	35	0.74(3)
60	1.2	1.52(2)	0.32(2)	40	0.79(5)
55	1.1	1.45(2)	0.35(2)	45	0.78(4)
50	1.0	1.36(2)	0.36(2)	50	0.71(4)
40	0.8	1.24(2)	0.44(2)	60	0.74(3)
30	0.6	1.13(2)	0.53(2)	70	0.75(3)
20	0.4	0.98(2)	0.58(2)	80	0.73(3)
10	0.2	0.87(2)	0.67(2)	90	0.74(2)
—	—	0.75(2)	0.75(2)	100	0.75(2)

Note. Standard deviations of the last figures are in parentheses (see text). (Subhydrate water) = (overall water) − (water from gypsum). To find x in $CaSO_4(H_2O)_x$:

$$x = \frac{100 \cdot (\text{subhydrate water})}{\%\ \text{subhydrate}}.$$

appears at temperatures greater than 330 K. By 374 K the gypsum phase had completely disappeared, leaving only the subhydrate phase. Beginning at 525 K, the AIII tunnel structure converts into the thermodynamically stable AII anhydrite. This phase transition should be of first order (two coexisting phases in the temperature range 525–625 K). Above 625 K only the AII phase was present.

Figure 2 shows a plot of the background intensity versus the temperature. At the beginning of the experiment, this intensity corresponds to $H_2O/CaSO_4 = 2$. The final background intensity from the completely dehydrated sample indicates the zero line. The point of inflection can be associated to the hemihydrate $CaSO_4(H_2O)_{0.5}$[1].

[1] An irregular behavior of the curve around scan No. 150 is due to a temporary breakdown of the furnace power supply during the diffraction experiments. As the dehydration was still going on (no lowering of the temperature), no falsification of the reaction occurred.

In order to detect the water content of the subhydrate structure the borderlines for the major structure types (gypsum, subhydrates/AIII, AII) were first determined using characteristic reflections from the diffraction patterns. These reflections (for example, 123 for gypsum, 100 for subhydrates/AIII, 200 and 002 for AII) should be of highest intensity and no coincidence with reflections of adjacent phases is allowed. The single reflection recordings were prepared by fitting Gaussian profiles to the measured line shapes. The corresponding results are given in Fig. 3.

Now, the different ratios of coexisting phases (from Fig. 3) were attached to the overall water content (from Fig. 2). The part of water from the gypsum phase, always considering two formula units H_2O per formula unit $CaSO_4$, was subtracted from the overall water content giving the water content of the subhydrate (see Table II). The mean values from two evaluations were taken.

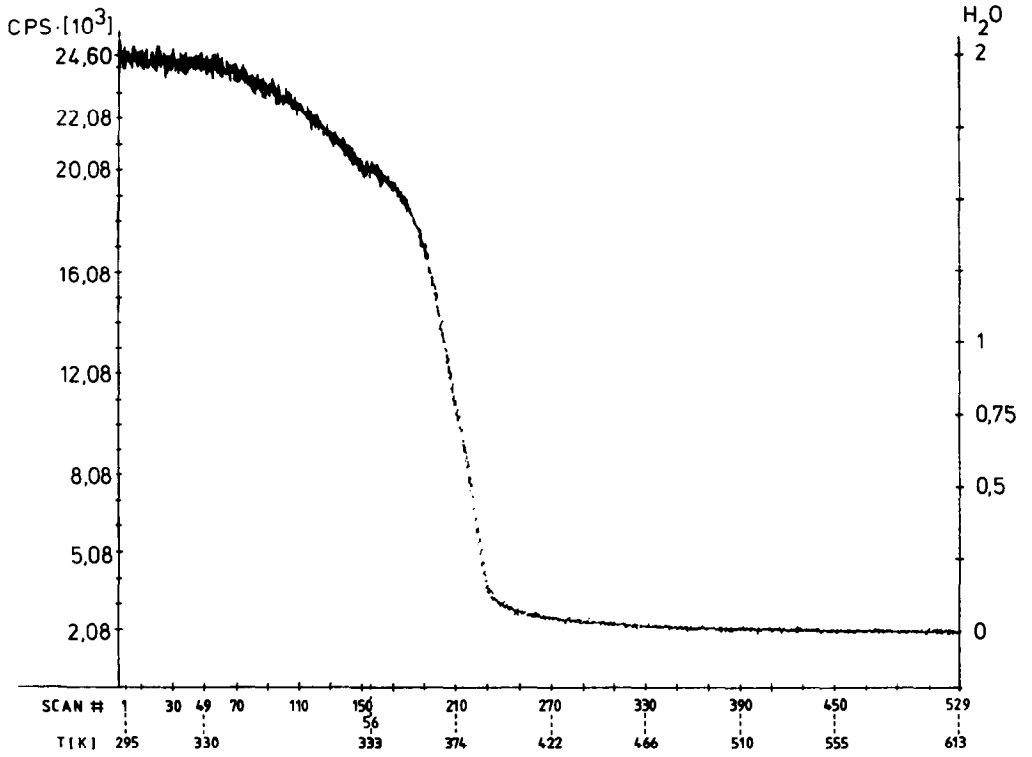

FIG. 2. Background intensity vs the temperature (from the NTD experiment). Scan No. denotes the single pattern.

Figure 4 shows the x-parameter for the water content of the subhydrate structure $CaSO_4(H_2O)_x$ versus the temperature. The values of the lower temperature region are rather inaccurate due to the fluctuations of the background intensity. The mean maximum water content of the subhydrate structure during this reaction is shown to be

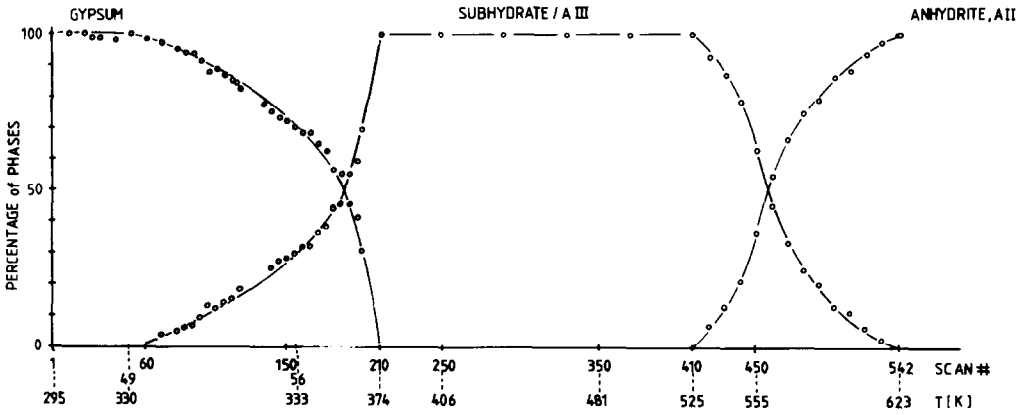

FIG. 3. Content of phases in percentage vs the temperature (from the NTD experiment).

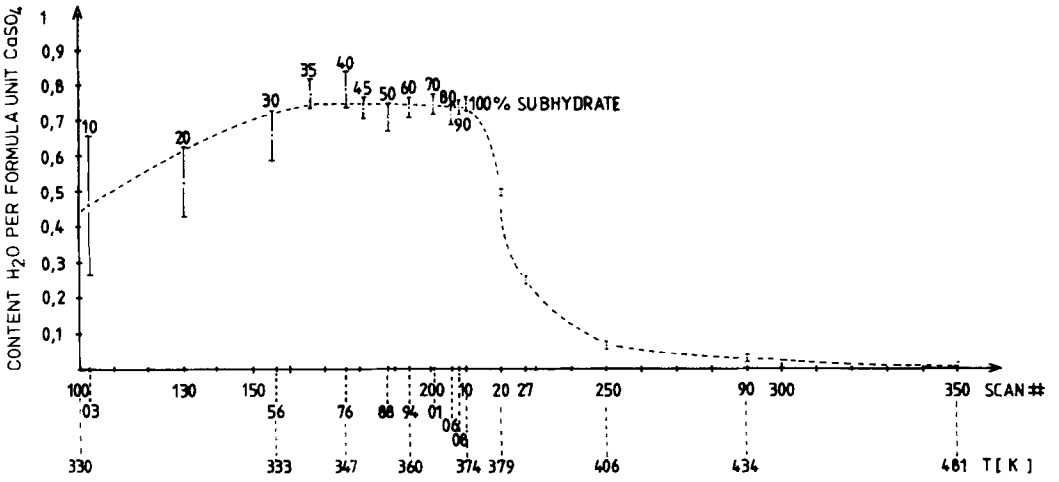

FIG. 4. Water content of the subhydrate structure $CaSO_4(H_2O)_x$ vs the temperature. The numbers at the error bars indicate the concentration of the subhydrate phase in the sample.

0.74(1) considering values from subhydrate concentrations ≧50%. With scan No. 210 (at 374 K) all the gypsum disappeared completely, from here the subhydrate tunnel structure exists exclusively. At this point the composition was calculated to $CaSO_4(H_2O)_{0.75}$. Continuously increasing dehydration finally yields AIII-$CaSO_4$ at scan No. 350 (481 K).

A refinement of the lattice constants of the subhydrate structure did not indicate significant changes in the unit cell dimensions with decreasing water content. As already pointed out (*12*), these data are strongly correlated with the state of hydration. This contradiction should be due to the poorer θ-resolution compared with X-ray Guinier data.

The dehydration reaction recorded with the X-ray Guinier device was much faster than found in the NTD experiment (Fig. 5). The chosen temperature of 335 K enabled the optimum kinetic for the recording of the gypsum-subhydrate conversion. A lattice refinement of the subhydrate structure in an early stage (G3) yielded the unit cell dimensions of the hemihydrate (*12*), indicating that the H_2O occupancy is not so high as found in the NTD experiment.

There is no evidence for a new phase between gypsum and the subhydrates from both experiments.

Discussion

All structures in the system $CaSO_4$–H_2O can be interpreted by a model of different packing of chains containing Ca^{2+} and SO_4^{2-} ions. In Fig. 6 one chain perpendicular to plane of paper is represented by a small circle. With this view one can easily recognize a layered structure (gypsum, the water molecules are interlayer guests), a tunnel structure (AIII-$CaSO_4$), and a rather closed packed array (AII-$CaSO_4$). In the subhydrates, the tunnels of the AIII structure are filled with water molecules. In the relatively stable hemihydrate one-half of all tunnel positions are occupied by guest molecules, each of them weakly connected to the framework by O_3SO–HOH–OSO_3 bonds (*13*). In highly loaded subhydrates, like in $CaSO_4$ $(H_2O)_{0.81}$ (*3*), in Ca $SO_4(H_2O)_{0.62}$ (*6*), or in $CaSO_4(H_2O)_{0.75}$,

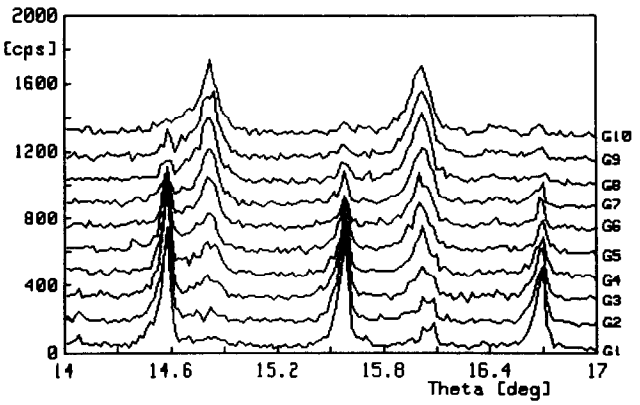

FIG. 5. Characteristic section of the Guinier diffraction patterns (Cu$K\alpha_1$ radiation). The dehydration reaction at a constant temperature of 335(1) K was recorded with 10 diffractograms in time intervals of 12 min. G1 starts with 100% gypsum, G10 ends with 100% subhydrate.

found in this NTD study, additional tunnel positions with no bonds to the matrix are filled with water molecules. These guest molecules can be moved more easily in a cooperative migration mechanism using empty sites (a monohydrate with completely filled tunnels is not known). The point of inflection at the hemihydrate state, observed in Figs. 2 and 4 and in corresponding thermogravimetric measurements (*1*, *8*), indicates the requirement for more energy to break the hydrogen bonds to the $CaSO_4$ framework in the course of further dehydration.

Subhydrates $CaSO_4(H_2O)_x$ with $x > 0.5$ can be obtained with high H_2O steam pressures only (*6*). In contrast to the Guinier experiment, where only a thin powder layer was fixed on a foil, the NTD experiment was performed in a rather big vessel. Although a vacuum was applied, the local H_2O steam pressures from the decomposing gypsum in the stuffed container were high enough to form this high tunnel occupation.

The hydration and dehydration mechanism within the tunnel structure is strongly topotactic (*1*), during the reaction the three-dimensional network of the host structure is conserved. Considering Fig. 6, the complete dehydration reaction of gypsum seems to be topotactic, too: At least one-dimensional structural elements (chains of alternating Ca^{2+} and SO_4^{2-} ions) should be conserved (*14*).

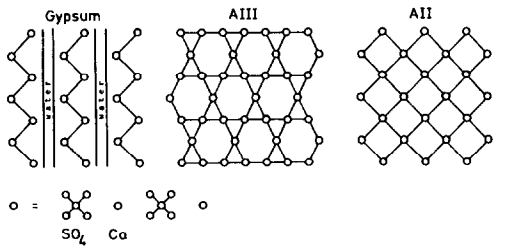

FIG. 6. Diagrams of structures in the system $CaSO_4$–H_2O. A chain of alternating Ca^{2+} and SO_4^{2-} ions is represented by a small circle (see text).

Conclusion

The existence of subhydrates $CaSO_4(H_2O)_x$ with $x > 0.5$ is evident. With high local H_2O steam pressures we found $x = 0.74$ in the NTD experiment.

The critical temperatures for decomposition and phase transition are a function of the bulk size (different local H_2O steam pressures).

There is no crystalline phase in between gypsum and the subhydrates.

Acknowledgments

Financial support by the Deutsche Forschungsgemeinschaft (Project A1, SFB 173) and the Fonds der Chemischen Industrie is gratefully acknowledged.

References

1. K. Reisdorf and W. Abriel, *Neues Jahrbuch Miner. Abh.* **157,** 35 (1987).
2. F. Wirsching, *in* "Ullmanns Enzyklopädie der Technischen Chemie," Verlag Chemie, Weinheim (1976).
3. W. Abriel, *Acta Crystallogr. C* **39,** 956 (1983).
4. N. N. Bushuev and V. M. Borisov, *Russ. J. Inorg. Chem.* **27,** 604 (1982).
5. H. J. Kuzel, *Neues Jahrbuch Miner. Abh.* **156,** 155 (1987).
6. H. J. Kuzel and M. Hauner, *Zement-Kalk-Gips* **40,** 628 (1987).
7. G. A. Lager, Th. Armbruster, F. J. Rotella, J. D. Jorgensen, and H. G. Hinks, *Amer. Mineral.* **69,** 910 (1984).
8. K. Reisdorf, Thesis, Universität Hannover (1987).
9. A. N. Christensen, M. S. Lehmann, and J. Pannetier, *J. Appl. Crystallogr.* **18,** 170 (1985).
10. J. Pannetier, *Chem. Scr. A* **26,** 131 (1986).
11. W. Abriel and U. Bismayer, *Phase Transitions* **15,** 49 (1989).
12. K. Reisdorf and W. Abriel, *Zement-Kalk-Gips* **41,** 356 (1988).
13. W. Abriel and R. Nesper, to be published.
14. L. S. Dent-Glasser, F. P. Glasser, and H. F. W. Taylor, *Q. Rev.* **16,** 343 (1962).